RESEARCH PAPER

Agonist-dependent cannabinoid receptor signalling in human trabecular meshwork cells

BT McIntosh, B Hudson, S Yegorova, CAB Jollimore and MEM Kelly

Department of Pharmacology and Laboratory for Retina and Optic Nerve Research, Dalhousie University, Halifax, Nova Scotia, Canada

Background and purpose: Trabecular meshwork (TM) is an ocular tissue involved in the regulation of aqueous humour outflow and intraocular pressure (IOP). CB_1 receptors (CB_1) are present in TM and cannabinoid administration decreases IOP. CB_1 signalling was investigated in a cell line derived from human TM (hTM).

Experimental approach: CB_1 signalling was investigated using ratiometric Ca^{2+} imaging, western blotting and infrared In-Cell Western analysis.

Key results: WIN55212-2, a synthetic aminoalkylindole cannabinoid receptor agonist (10–100 μM) increased intracellular Ca^{2+} in hTM cells. WIN55,212-2-mediated Ca^{2+} increases were blocked by AM251, a CB_1 antagonist, but were unaffected by the CB_2 antagonist, AM630. The WIN55,212-2-mediated increase in $[Ca^{2+}]_i$ was pertussis toxin (PTX)-insensitive, therefore, independent of $G_{i/o}$ coupling, but was attenuated by a dominant negative $G\alpha_{q/11}$ subunit, implicating a $G_{q/11}$ signalling pathway. The increase in $[Ca^{2+}]_i$ was dependent upon PLC activation and mobilization of intracellular Ca^{2+} stores. A PTX-sensitive increase in extracellular signal-regulated kinase (ERK1/2) phosphorylation was also observed in response to WIN55,212-2, indicative of a $G_{i/o}$ signalling pathway. CB_1-$G_{q/11}$ coupling to activate PLC-dependent increases in Ca^{2+} appeared to be specific to WIN55,212-2 and were not observed with other CB_1 agonists, including CP55,940 and methanandamide. CP55940 produced PTX-sensitive increases in $[Ca^{2+}]_i$ at concentrations ≥ 15 μM, and PTX-sensitive increases in ERK1/2 phosphorylation.

Conclusions and implications: This study demonstrates that endogenous CB_1 couples to both $G_{q/11}$ and $G_{i/o}$ in hTM cells in an agonist-dependent manner. Cannabinoid activation of multiple CB_1 signalling pathways in TM tissue could lead to differential changes in aqueous humour outflow and IOP.

British Journal of Pharmacology (2007) **152**, 1111–1120; doi:10.1038/sj.bjp.0707495; published online 8 October 2007

Introduction

In humans, intraocular pressure (IOP) is determined by the secretion of aqueous humour by the ciliary epithelium and aqueous humour outflow via the trabecular and uveoscleral pathways. The trabecular meshwork (TM), leading to Schlemm's canal, is located in the anterior chamber of the eye, and represents the major site of outflow resistance. In support of a role in regulating IOP, alterations in the morphology and function of TM cells are associated with changes in outflow resistance. This has led to an interest in

these cells as therapeutic targets in the treatment of primary open angle glaucoma, a neurodegenerative optic nerve disease in which a primary risk factor is elevated IOP (Kaufman *et al.*, 1999; Ferrer, 2006; Tan *et al.*, 2006).

In the early 1970s, it was shown that smoking *Cannabis sativa* (marijuana) significantly lowered IOP (Hepler and Frank, 1971). Since then, numerous studies have shown that systemic or topical administration of cannabinoids decreases IOP (Tomida *et al.*, 2004). The physiological effects of cannabinoids, such as Δ^9-tetrahydrocannabinol, were initially attributed to nonspecific disruption of the plasma membrane based on their high lipid solubility. However, the cloning of two G-protein-coupled receptors, CB_1 and CB_2 (Matsuda *et al.*, 1990; Munro *et al.*, 1993), that specifically bind cannabinoids, precipitated the discovery of the endocannabinoid system, consisting of cannabinoid receptors,

endogenous endocannabinoids and the enzymes required for their synthesis and degradation (Piomelli, 2003; Jonsson *et al*., 2006).

CB$_1$ cannabinoid receptors (CB$_1$) are present in ocular tissues of both the inflow and outflow pathways, including the TM (Straiker *et al*., 1999; Porcella *et al*., 2000; Stamer *et al*., 2001). The functional relevance of CB$_1$ in TM tissue is still unclear, although activation of CB$_1$ has been found to activate Ca^{2+}-sensitive K$^+$ channels in human TM cells and relax bovine TM tissue strips (Stumpff *et al*., 2005), both of which may contribute to alterations in outflow resistance and IOP.

The purpose of the present study was to investigate the pharmacology of endogenous CB$_1$ activation by cannabinoid ligands in cells derived from the human trabecular meshwork (hTM). Cannabinoid receptor ligands are a structurally diverse class of compounds that include four main groups: (1) classical cannabinoids are dibenzopyrene derivatives from *C. sativa* or synthetic analogues, (2) non-classical cannabinoids are structural analogues of the classical group that lack a pyran ring, (3) aminoalkylindoles are synthetic compounds with a unique pharmacophore and (4) eicosanoids are derivatives of arachidonic acid and include the endogenous cannabinoid receptor ligands (Pertwee, 2005b).

Cannabinoid activation of CB$_1$ has been shown to result in preferential coupling to the G$_{i/o}$ family of heterotrimeric G-proteins and is associated with inhibition of adenylyl cyclase and voltage-gated Ca^{2+} channels (N, P/Q type), and activation of inwardly rectifying K$^+$ channels and the mitogen-activated protein kinase (MAPK) cascade (Howlett, 2005). In addition, a number of studies have now provided evidence demonstrating that the CB$_1$ receptor is capable of pleiotropism, or coupling to multiple families of heterotrimeric G-proteins. For example CB$_1$ can couple to both G$_{i/o}$ and G$_s$ to inhibit and stimulate the activity of adenylyl cyclase (Felder *et al*., 1995; Glass and Felder, 1997; Bonhaus *et al*., 1998). In each case, G$_{i/o}$/G$_s$ coupling efficiency varied in an agonist-dependent manner, an observation frequently referred to as functional selectivity (Urban *et al*., 2007). Agonist-dependent cannabinoid signalling has also been demonstrated with respect to CB$_1$ activation of G$_i$ and G$_o$ proteins (Glass and Northup, 1999). Taken together, these observations suggest that the effects of individual CB$_1$ agonists may be determined in part by receptor/G-protein pleiotropism providing for differential alterations in cellular function.

More recently, it was revealed that WIN55212-2, a full agonist at both CB$_1$ and CB$_2$, can evoke a gradual [Ca^{2+}]$_i$ increase in CB$_1$-expressing HEK293 cells. This increase in [Ca^{2+}]$_i$ was shown to be a result of CB$_1$-coupling to G$_{q/11}$ and was specific to WIN55212-2, with other CB$_1$ agonists unable to produce this response (Lauckner *et al*., 2005). In contrast, pertussis toxin (PTX)-sensitive signal transduction is well documented with CB$_1$ agonists, suggesting the possibility of agonist-specific G$_{q/11}$/G$_{i/o}$ pleiotropism. Currently, it remains unclear if CB$_1$ is capable of G$_{q/11}$/G$_{i/o}$ pleiotropy or is a property of endogenously expressed CB$_1$ receptors.

In the present study, CB$_1$ signalling was examined in hTM cells using cannabinoid agonists from different structural classes including the aminoalkylindole, WIN55212-2, the

non-classical CB$_1$ agonist, CP55940 and the eicosanoid methanandamide. Our results demonstrate agonist-dependent pleiotropic coupling of endogenous CB$_1$ receptors to G$_{q/11}$ and G$_{i/o}$ proteins to evoke increases in [Ca^{2+}]$_i$ and extracellular signal-regulated kinases 1 and 2 (ERK1/2) phosphorylation, respectively. Endogenous CB$_1$ coupling to PTX-insensitive G$_{q/11}$ in hTM cells to increase [Ca^{2+}]$_i$ was observed with the aminoalkylindole agonist, WIN55212-2, but not with the non-classical or eicosanoid CB$_1$ agonists, which mediated their actions via PTX-sensitive G$_{i/o}$-coupled pathways. This disparity in CB$_1$ signalling may represent a means by which the aminoalkylindole class of cannabinoid agonists can differentially regulate aqueous humour outflow and IOP.

Methods

Cell culture

Cells from the hTM5 cell line were provided by Alcon Research (Fort Worth, TX, USA). Cells were grown in BD Falcon culture flasks (VWR, Missisauga, ON, Canada) in Dulbecco's modified Eagle's medium with 50 µg ml^{-1} gentamicin (Sigma-Aldrich Canada Ltd, Oakville, ON, Canada) supplemented with 10% fetal bovine serum (Hyclone, Logan, UT) in an atmosphere containing 5% CO$_2$ and 95% air at 37°C. Cells were passaged every 3 days using 1X Accutase (Cedarlane Laboratories, Burlington, ON, Canada).

Calcium imaging

hTM cells were seeded onto 35 mm/12 mm glass-bottom culture dishes (Warner Instruments, Hamden, CT, USA) and grown for 36–48 h in Dulbecco's modified Eagle's medium with 10% fetal bovine serum. Serum was removed 12–24 h prior to imaging. Calcium indicator loading solution containing 5 µM Fura-2 AM dispersed in 0.1% pluronic F-127 (Invitrogen Canada Inc., Burlington, ON, Canada) was prepared in Kreb's ringer buffer containing (in mM): 125 NaCl, 4.5 KCl, 1.8 CaCl$_2$, 0.8 MgCl$_2$, 10 D-glucose, 10 Hepes, 0.5 Na$_2$HPO$_4$ and 5.0 NaHCO$_3$, pH 7.4. Media were removed and replaced with 1 ml of loading solution; cells were then incubated in the dark for 40–45 min at 37°C. Dishes were subsequently transferred to a microscope chamber and superfused for 10 min in Kreb's ringer buffer. The superfusion rate was 0.4–0.6 ml min^{-1} and solutions were passed through a pre-heater (SF-28 Inline Heater, TC-324B controller; Warner Instruments) that allowed the bath temperature to remain at 34–37°C. Fura-2 fluorescence was produced by excitation from a 100 W xenon arc-lamp (Lambda LS, Sutter Instrument Company, Novato, CA, USA) and the appropriate filter set (excitation at 340 or 380 nm; emission 510 nm; dichroic > 430 nm; Omega Optical, Brattleboro, VT, USA). Alternation between 340 and 380 nm was controlled by a Lamda 10–2 optical filter changer (Sutter Instrument Company) with an exposure time of 0.3 s for each filter set. The excitation illumination was passed through −1.0 log neutral density filter to reduce photodamage. Images were captured using a SenSys cooled charge-coupled device camera (Roper Scientific Inc., Tucson, AZ, USA) fitted to a Nikon UM-2

fluorescence microscope (Nikon Canada Inc., Mississauga, ON, Canada) and employing a water immersion $40 \times$ objective. Ratiometric values were derived from the cytosolic area and averaged within the delimited area using Imaging Work-Bench 5.1 (Molecular Devices, Sunnyvale, CA, USA). Measurements were performed every 20–60 s during washing and 2–10 s intervals upon drug application. The peak amplitude of the Ca^{2+} movement was determined by subtracting the mean basal 340/380 nm ratio from the maximum observed 340/380 nm ratio following exposure to the various agonists. Baseline values were recorded for 3 min before the addition of agonist and following a 10 min wash to remove excess fura-2 from the bath solution. Background for 340 and 380 nm was subtracted prior to baseline recordings. Antagonists and inhibitors were perfused for 10 min prior to co-application of antagonist/ inhibitor with cannabinoid receptor agonist for a further 5 min.

In-Cell Western analysis

Activation of the MAPK pathway was assessed by measuring phosphorylation of extracellular signal-regulated kinases 1 and 2 (pERK1/2). In-Cell Western analysis was conducted using the Odyssey Infrared Imaging System (LI-COR Biotechnology, Lincoln, NE, USA). Cells were grown in a 96-well plate for 48–72 h before the experiments were started. Twenty-four hours prior to experiments, the culture media was replaced with serum-free Dulbecco's modified Eagle's medium. Cells were exposed to drugs for 5 min and then fixed in 4% paraformaldehyde for 1 h at room temperature. After the cells had been made permeable for 1 h in phosphate-buffered saline (PBS) containing 0.1% Triton X-100, cells were blocked for 2 h in blocking buffer (1% bovine serum albumin in PBS supplemented with 0.1% Tween 20). An anti-phospho ERK1/2 primary antibody raised in rabbit (Santa Cruz Biotechnology Inc., Santa Cruz, CA, USA) was diluted in blocking buffer and applied to the cells overnight at 4°C. After being washed with PBS supplemented with 0.1% Tween 20 (PBST), cells were incubated with an anti-rabbit IR800CW-conjugated secondary antibody (Rockland Immunochemicals Inc., Gilbertsville, PA, USA). Cells were then washed again with PBST and incubated with an anti-total ERK2 antibody raised in goat (Santa Cruz Biotechnology Inc., Santa Cruz, CA, USA) diluted in blocking buffer for 1 h at room temperature. After being washed with PBST, cells were then incubated in an anti-goat Alexa Fluor680-conjugated secondary antibody (Invitrogen Canada Inc.). Following this incubation, cells were finally washed with PBST, followed by single washes with PBS and dH$_2$O. The 96-well plates were then inverted and pressed against paper towel to remove as much of the dH$_2$O as possible before being left to dry. Once the cells were dry, the plates were scanned using the Odyssey infrared imaging system (LI-COR Biotechnology).

Cell transfection

A dominant-negative G$_{q/11}$ α-subunit (DNG$_{\alpha q}$) construct was obtained from the UMR cDNA Resource Center (Rolla, MO,

USA; www.cdna.org) and subcloned into the *Nhe*I and *Xho*I sites of a pIRES2-enhanced green fluorescent protein (EGFP) vector (BD Biosciences Clontech, Mountain View, CA, USA). hTM cells were transfected with either the empty pIRES2-EGFP or pIRES2-EGFP-DNG$_{\alpha q}$ vectors using Lipofectamine 2000 (Invitrogen Canada Inc.), according to manufacturer's instructions. Cells were seeded onto coverslips 24 h following the transfection and subsequently used for imaging. The mutant protein contains two point mutations (Q209L and D277N) that alter α-subunit-binding preference from guanine to xanthine nucleotides. The mutant retains the ability to interact with the receptor, but a lack of cytosolic xanthine prevents activation, allowing it to act as a competitive inhibitor of wild-type G$_{q/11}$ proteins (Yu and Simon, 1998).

Transfection of CB$_1$R into hTM

CB$_1$ over expressing hTM cell line was generated by transfecting human CB$_1$ receptor cDNA from UMR cDNA Resource Center (www.cdna.org) using Fugene 6 (Roche, Laval, QC, Canada) according to the manufacturer's instructions. A stably transfected clone was selected by Geneticin G-418 (Invitrogen Canada Inc.) 1 mg ml^{-1}.

Immunocytochemistry

hTM cells were grown on 12 mm cover slips for 36–48 h. Media were removed and cells were washed once with PBS and then fixed with 4% paraformaldehyde for 5 min at room temperature. Fixed cells were blocked with 10% normal goat serum in PBS for 1 h at room temperature with constant agitation, followed by overnight incubation (4°C) with primary anti-human CB$_1$ receptor rabbit polyclonal immunoglobulin G (IgG) or a 1:1 mixture of the primary antibody with blocking peptide (Cayman Chemical, Ann Arbor, MI, USA). Finally, cells were incubated with AlexaFluor 546 goat anti-rabbit IgG (Invitrogen Canada Inc.) for 1 h at room temperature. At each stage of the procedure, cells were washed 4×5 min with PBS. Immunostaining was observed using a laser scanning Nikon confocal microscope (Nikon Canada Inc.).

Immunoblotting

Cultured hTM cells were washed three times in ice-cold PBS solution (140 mM NaCl, 15 mM KH$_2$PO$_4$ (pH 7.2), 2.7 mM KCl), and proteins were extracted with lysis buffer containing 50 mM Tris-HCl, pH 7.4, 150 mM NaCl, 1 mM EDTA, 1% (v v^{-1}) NP-40, 1 mM Na$_3$VO$_4$, 0.25% Na-deoxycholate, 1 mM PMSF, 1 mM NaF, 1 µg ml^{-1} each of aprotinin, pepstatin and leupeptin. Lysates were centrifuged at 16 060 *g* for 5 min at 4°C. The supernatant was immediately transferred to a fresh 1.5 ml tube, and the protein concentration was measured by Bio-Rad Protein Assay (Bio-Rad Laboratories, Hercules, CA, USA). Twenty micrograms of protein from cell lysates were subjected to SDS-polyacrylamide gel electrophoresis and transferred to a HyBond-c super membrane (GE Healthcare Life Sciences, Piscataway, NJ, USA) or Immun-Blot polyvinylidene difluoride membrane (Bio-Rad Laboratories). Proteins were transferred using Mini Trans-Blot electrophoretic

transfer cell (Bio-Rad Laboratories) according to the manufacturer's protocol. Precision Plus Protein Dual Color Standards were used as molecular weight markers (Bio-Rad Laboratories). The primary antibody was rabbit anti-human cannabinoid CB$_1$ receptor polyclonal IgG diluted 1:2000 in TBST/1% bovine serum albumin buffer (Cayman Chemical). The secondary antibody was horseradish peroxidase-conjugated goat anti-rabbit IgG diluted 1:5000 in TBST/1% bovine serum albumin buffer (Vector Laboratories Inc., Burlingame, CA, USA). Proteins were visualized using the ECL detection system, according to the instructions of the manufacturer (GE Healthcare Life Sciences), using autoradiography film (LabScientific, Livingston, NJ, USA). CB$_1$ blocking peptide was obtained from Cayman Chemical. Anti-human α-tubulin diluted 1:15000 (Cedarlane Laboratories) was used as a loading control for CB$_1$ immunoblotting.

Reverse transcriptase-PCR
Total cellular mRNA was isolated from cultured normal hTM cells and human CB$_1$ over expressing hTM cells (unpublished data) using Micro PolyA Pure kit (Applied Biosystems Canada, Streetsville, ON, Canada), resuspended in RNase-free water (Applied Biosystems Canada) and treated with DNase I (Invitrogen Canada Inc.). Isolated mRNA was reverse transcribed using RETROscript™ kit (Applied Biosystems Canada) using poly (dT) primer, as described by the manufacturer's instructions. Aliquots, 2 μl, from each cDNA reaction were subjected to PCR, using primer sets for detecting CB$_1$ or β-actin and JumpStart Taq DNA Polymerase (Sigma-Aldrich, Oakville, ON, Canada). Forward and reverse primers for CB$_1$ were (5′–3′) GACGTGTGGATGATGATGCTCTTC and TGCAGGCCTTCCTACCACTTCATC, respectively (Invitrogen Canada Inc.). Forward and reverse primers for β-actin were (5′–3′) CTCTTCCAGCCTTCCTTCCT and CAGGGCAGTGATCTCCTTCT, respectively. The sizes of the amplification products were 510 and 180 bp, respectively. Conditions for PCR reactions were 94° C for 1 min, 54° C for 1 min and 72° C for 1 min. PCR amplification was conducted for 32 cycles. Reverse transcriptase-PCR products were analysed by agarose gel electrophoresis and digital imaging of the ethidium bromide-stained gel.

Materials
Thapsigargin was obtained from Alomone Labs (Jerusalem, Israel). PTX, pluronic f-127, cyclopiazonic acid, U73122 (1-[6-[((17β)-3-methoxyestra-1,3,5(10)-trien-17-yl)amino]hexyl]-1H-pyrrole-2,5-dione) and U73433 (1-[6-[((17β)-3-methoxy-estra-1,3,5(10)-trien-17-yl)amino]hexyl]-2,5-pyrrolidinedione) were from Calbiochem (San Diego, CA, USA). (R)-(+)-WIN55,212-2 mesylate salt ((R)-(+)-[2,3-dihydro-5-methyl-3-(4-morpholinylmethyl)pyrrolo[1,2,3-de]-1,4-benzoxazin-6-yl]-1-naphthalenylmeth anone mesylate), CP55940 ((−)-cis-3-[2-hydroxy-4-(1,1-dimethylheptyl)phenyl]-trans-4-(3-hydroxy-propyl)cyclohexanol), anadamide, AM630 (6-iodo-2-methyl-1-[2-(4-morpholinyl)ethyl]-1H-indol-3-yl](4-methoxyphenyl) methanone) were from Tocris Cookson (Ellisville, MO, USA). AM251 (N-(piperidin-1-yl)-5-(4-iodophenyl)-1-(2,4-dichloro-phenyl)-4-methyl-1H-pyrazole-3-carboxamide) was obtained

from Caymen Chemical (Ann Arbor, MI, USA). R(+)-methanandamide, dimethylsulphoxide (DMSO), Dulbecco's modified Eagle's medium and gentamicin were from Sigma-Aldrich.

Statistical analysis and curve fitting
All data are presented as mean ± s.e.m. Statistical analysis and curve fitting (sigmoidal dose-response, variable slope) were performed using GraphPad Prism v.4 (GraphPad Software Inc., San Diego, CA, USA). Significance was determined using analysis of variance with Dunnett's or Tukey's multiple comparison test when the number of treatment groups exceeded three and unpaired Student's *t*-test when two treatment groups were compared. $P < 0.05$ was considered statistically significant.

Results

CB$_1$ expression in hTM cells
Immunocytochemistry, western blot analysis and reverse transcription-PCR were used to demonstrate CB$_1$ expression in hTM cells. Positive fluorescent staining was obtained in cells exposed to primary anti-CB$_1$ antibody (Figure 1a). Cells incubated with both blocking peptide and anti-CB$_1$ antibody (1:1) showed only a low level of fluorescence. Cells exposed to only the secondary antibody revealed no significant
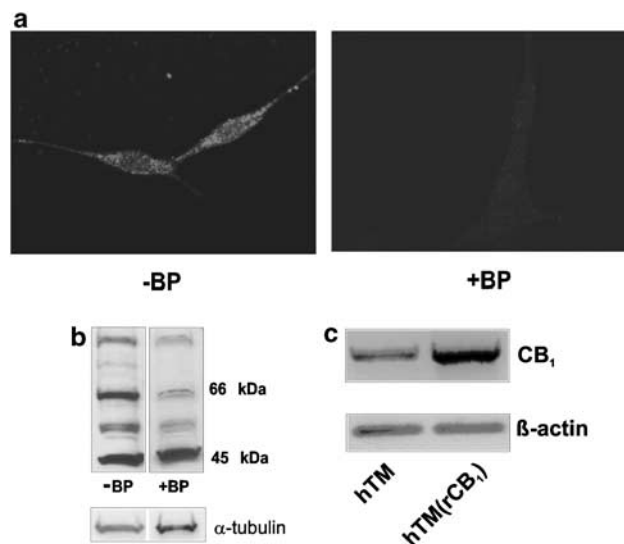
Figure 1 CB$_1$ receptor is present in hTM cells. (**a**) hTM cells labelled with anti-human CB$_1$ rabbit polyclonal IgG (−BP), and hTM cells treated with 1:1 mixture of anti-CB$_1$ rabbit polyclonal IgG with blocking peptide (+BP). AlexaFluor 546 goat anti-rabbit IgG was used as the secondary antibody. (**b**) CB$_1$ was detected using western blot analysis. Four prominent bands are present, ranging from 97 to 45 kDa (−BP), three of which were substantially reduced following pre-absorption with a blocking peptide (+BP). CB$_1$ was detected at the expected size for this antibody (66–64 kDa). α-Tubulin was used as a loading control. (**c**) Reverse transcription-PCR was performed using normal hTM cells and hTM(rCB$_1$) cells, which stably over-express human CB$_1$. β-Actin was used as a loading control. htm, human trabecular meshwork; IgG, immunoglobulin G.

CB$_1$ signalling in human trabecular meshwork
BT McIntosh *et al*
1115

fluorescence (data not shown). CB$_1$ receptor protein was also detected using western blot analysis. Several bands are visible on the blot, three of which were reduced following pre-absorption with a blocking peptide (1:1). The intensity of the band at 66 kDa was greatly reduced ($>$65%) by the blocking peptide (Figure 1b), consistent with the expected size of CB$_1$ for this antibody. CB$_1$ mRNA was detected using reverse transcription-PCR (Figure 1c) in normal hTM cells and in hTM cells stably over-expressing human CB$_1$. The level of CB$_1$ transcript is enhanced in the over-expressing cell line, confirming the identity of the amplicon.

WIN55,212-2 activates CB$_1$ to increase [Ca^{2+}]$_i$

Fluorescent ratiometric Ca^{2+} imaging with fura-2 was used to measure changes in cytosolic Ca^{2+}. Perfusion of hTM cells with WIN55,212-2 produced an increase in [Ca^{2+}]$_i$, as measured by an increase in fura-2 ratio (340/380 nm). Figure 2a shows images of representative hTM cells loaded with fura-2 before (baseline) and after 5 min exposure to 10 μM WIN55,212-2. WIN55,212-2 caused an increase in the ratio of fluorescence measured at 340/380 nm. The graph in Figure 2b shows the fura-2 ratio for 15 cells exposed to 10 μM WIN55,212-2. The WIN55,212-2-mediated [Ca^{2+}]$_i$ increase

occurred slowly and was sustained for 17.2 ±1.4 min. Figure 2c shows mean peak fura-2 ratio for 0.1–100 μM concentrations of WIN55,212-2, CP55940 and methananda-mide. WIN55,212-2 significantly increased [Ca^{2+}]$_i$ ($P<0.01$) at concentrations of 10 μM ($n=28$), 30 μM ($n=28$) and 100 μM ($n=17$) compared to 0.1 and 0.5% DMSO ($n=15$ and 22, respectively). CP55940 significantly increased [Ca^{2+}]$_i$ at concentrations of 15 μM ($n=18$), 30 μM ($n=38$) and 100 μM ($n=47$), in comparison with DMSO controls. The eicosanoid, methanandamide, failed to evoke a significant increase in [Ca^{2+}]$_i$ at all concentrations tested.

WIN55,212-2 is a nonspecific cannabinoid receptor agonist and has significant activity at both the CB$_1$ and CB$_2$ receptors (Pertwee, 2005b). To confirm that WIN55,212-2 activates CB$_1$ to increase [Ca^{2+}]$_i$ in hTM cells, the cells were treated with AM251, a CB$_1$ receptor inverse agonist, or AM630, a CB$_2$ antagonist (Figure 2). A 5 min pre-exposure to AM251, followed by co-application of either 1 μM ($P<0.01$, $n=24$) or 10 μM AM251 ($P<0.01$, $n=20$) together with 10 μM WIN55,212-2, produced a reduction of the WIN55,212-2-mediated increase in [Ca^{2+}]$_i$ compared with controls (no inhibitor; $n=28$). In contrast, the WIN55,212-2-mediated Ca^{2+} increase was not affected by CB$_2$ inhibition with AM630 (1 μM, $n=26$; 10 μM, $n=18$).
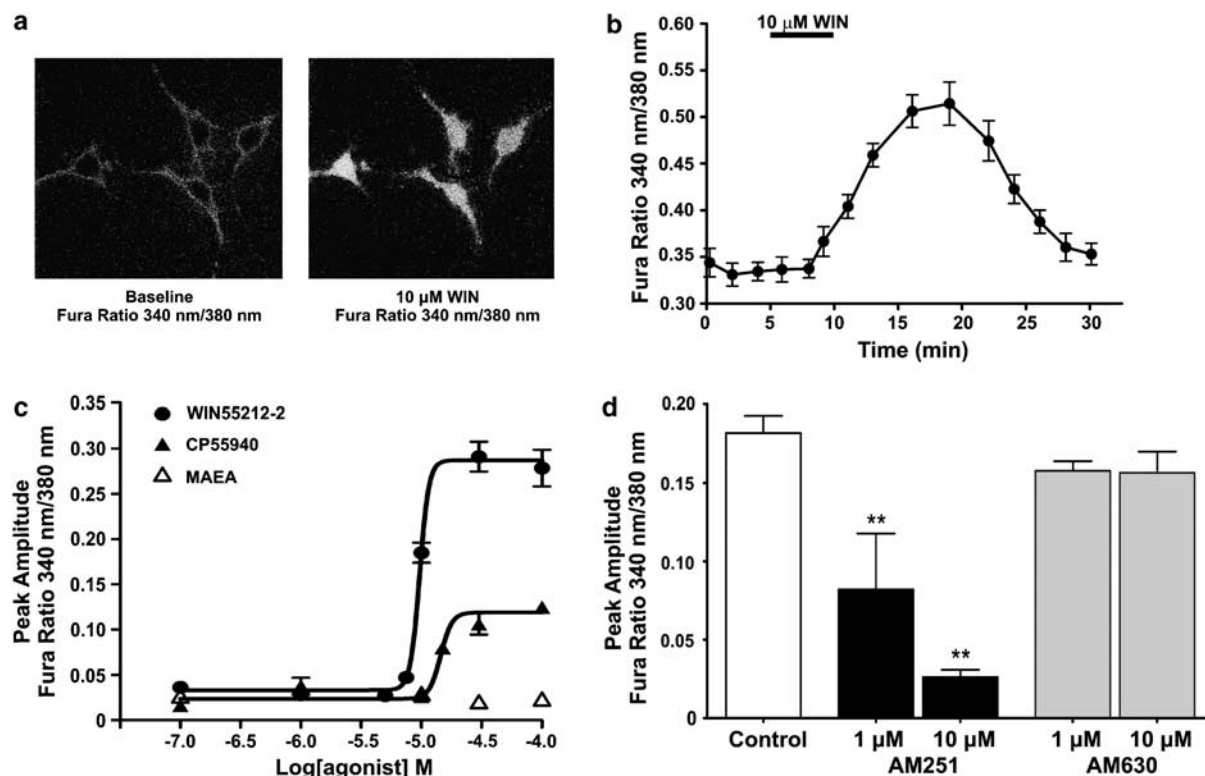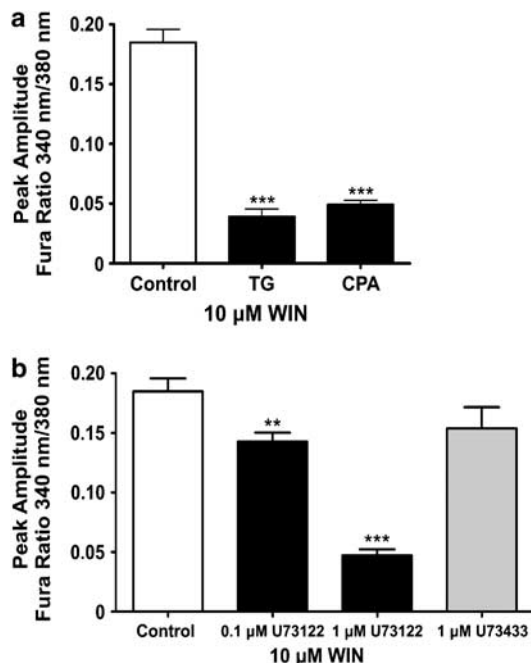

Figure 2 WIN55212-2 and CP55940 induce an increase in [Ca^{2+}]$_i$ in hTM cells. (**a**) Ratiometric calcium imaging of hTM cells in the absence and presence of 10 μM WIN55,212-2. The representative image was captured at the peak increase in [Ca^{2+}]$_i$ (18 min). (**b**) hTM cells were treated with 10 μM WIN55,212-2 for 5 min. WIN55,212-2 induces an increase in [Ca^{2+}]$_i$, represented as an increase in the fura-2 ratio (340/380 nm), that is sustained for 17.2 ±1.4 min. (**c**) Mean Ca^{2+} increases at concentrations of 0.1–100 μM WIN55,212-2, CP55940 and methananadamide. (**d**) The WIN55,212-2-induced increase in [Ca^{2+}]$_i$ is mediated by the CB$_1$ receptor. Graph shows the mean peak amplitude of the Ca^{2+} increase for 10 μM WIN55,212-2 in the absence or presence of AM251 (1 μM, $n=24$; 10 μM, $n=20$), a specific CB$_1$ receptor antagonist, or AM630 (1 μM, $n=26$; 10 μM, $n=18$), a specific CB$_2$ receptor antagonist. *$P<0.05$ and **$P<0.01$ in comparison with 10 μM WIN55,212-2 control (no inhibitor).

WIN55,212-2-mediated [Ca^{2+}]$_i$ increase requires release from internal stores

The WIN55,212-2-mediated [Ca^{2+}]$_i$ increase resulted from a mobilization of intracellular Ca^{2+} stores (Figure 3a). We used thapsigargin and cyclopiazonic acid, irreversible and reversible inhibitors, respectively, of the sarcoplasmic/endoplasmic reticulum Ca^{2+} ATPase pumps to deplete internal Ca^{2+} stores. Inhibition of the sarcoplasmic/endoplasmic reticulum Ca^{2+} ATPase pumps prevents Ca^{2+} from being sequestered in the endoplasmic reticulum and it is gradually lost from the cell via passive leakage into the cytosol and subsequent plasma membrane extrusion (Treiman et al., 1998). Following depletion of internal stores, WIN55,212-2 was no longer able to induce Ca^{2+} mobilization and produce a significant increase in [Ca^{2+}]$_i$ (thapsigargin, $P < 0.001$, $n = 23$; cyclopiazonic acid, $P < 0.001$, $n = 29$; control, $n = 28$), demonstrating the requirement for intact internal stores in the WIN55,212-2-mediated increase in [Ca^{2+}]$_i$.

WIN55,212-2-mediated increase in [Ca^{2+}]$_i$ is dependent upon activation of PLC

Activation of phospholipase C (PLC) results in the hydrolysis of phosphatidyl inositol (4,5)-bisphosphate and the production of two intracellular messengers, inositol (1,4,5)-triphosphate and diacylglycerol. The generation of inositol (1,4,5)-triphosphate and the activation of inositol (1,4,5)-triphosphate
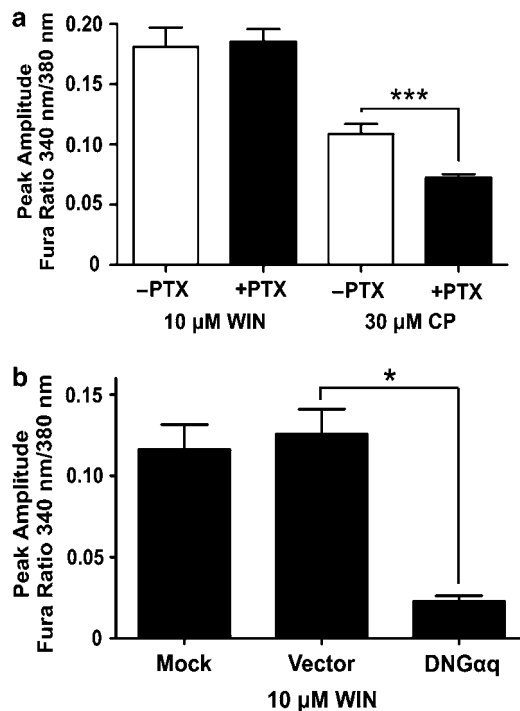
receptors regulates the release of Ca^{2+} from internal stores in many cell types (Berridge, 1993; Pinton et al., 1998). Figure 3b demonstrates that the WIN55,212-2-mediated increase in [Ca^{2+}]$_i$ is dependent upon activation of PLC. We used the aminosteroid, U73122, a commonly used inhibitor of PLC, and found that it reduced the peak amplitude of the WIN55,212-2-mediated Ca^{2+} increase, with a reduction of $23 \pm 4.1\%$ ($P < 0.05$, $n = 22$) and $74.4 \pm 2.8\%$ ($P < 0.01$, $n = 22$) compared to controls, with 0.1 and 1 μM U73122, respectively. U73343, the inactive analogue of U73122, had no significant effect upon the release of Ca^{2+} ($P > 0.05$, $n = 18$). A dose of 1 μM U73122 was not exceeded as this compound has been shown to release Ca^{2+} from internal stores at higher doses (Willems et al., 1994; Mogami et al., 1997; Jan et al., 1998).

WIN55,212-2-mediated [Ca^{2+}]$_i$ increase is PTX-insensitive and dependent upon CB$_1$-G$_{q/11}$ coupling

To evaluate the role of G$_{i/o}$ proteins in transducing the WIN55,212-2-mediated Ca^{2+} increase, cells were pretreated with 500 ng ml^{-1} of PTX for 20–24 h. PTX pretreatment did not significantly alter the increase in [Ca^{2+}]$_i$ following exposure to 10 μM WIN55,212-2 relative to control


Figure 3 [Ca^{2+}]$_i$ increase involves phospholipase C and mobilization of Ca^{2+} stores. (a) The mean peak amplitude of the WIN55,212-2-induced [Ca^{2+}]$_i$ increase following pretreatment with the sarco/endoplasmic reticulum calcium ATPase inhibitors thapsigargin (TG) ($n = 23$) and cyclopiazonic acid (CPA) ($n = 29$). (b) The mean peak amplitude of the WIN55,212-2-induced [Ca^{2+}]$_i$ increase in the presence of 0.1 μM ($n = 22$) and 1 μM ($n = 22$) U73122, a phospholipase C inhibitor, and 1 μM U73343 ($n = 18$), the inactive analogue of U73122. **$P < 0.01$ and ***$P < 0.001$ in comparison with 10 μM WIN55,212-2 control (no inhibitor).

Figure 4 WIN55,212-2(WIN)-mediated [Ca^{2+}]$_i$ increase is a result of CB$_1$-G$_{q/11}$ signal transduction. (a) The peak amplitude of the WIN and CP55940 (CP)-induced [Ca^{2+}]$_i$ increases in hTM cells that had been incubated in 500 ng ml^{-1} of pertussis toxin for 20–24 h (+PTX) in comparison to control cells (−PTX). WIN: −PTX, $n = 28$; +PTX, $n = 23$. CP: −PTX, $n = 38$; +PTX, $n = 25$. (b) The peak amplitudes of the WIN-induced [Ca^{2+}]$_i$ increases in hTM cells receiving a mock transfection ($n = 12$), cells receiving the empty vector ($n = 3$) and cells expressing a dominant-negative G$_{q/11}$ α-subunit (DNG$_{αq}$) protein ($n = 6$). *$P < 0.05$ in comparison with pIRES2-enhanced green fluorescent protein expressing cells.

(Figure 4a). These results suggest that the observed WIN55,212-2-mediated Ca^{2+} mobilization did not depend on CB$_1$-G$_{i/o}$ coupling. In contrast to WIN55,212-2, there was a significant reduction in the peak amplitude ($P<0.001$) and area under curve ($P<0.01$) for the CP-mediated Ca^{2+} increase following PTX pretreatment ($n=25$), suggesting that the increase involves a PTX-sensitive G$_{i/o}$-coupled pathway (Figure 4a).

Many G-protein-coupled receptors that are linked to PLC activation and Ca^{2+} mobilization couple to G$_{q/11}$ (Werry et al., 2003). Due to the PTX insensitivity of the WIN55,212-2-mediated Ca^{2+} transient, the involvement of G$_{q/11}$ was investigated. Transient transfection of hTM cells was carried out with a DNG$_{\alpha q}$ subcloned into the bicistronic pIRES2-EGFP vector. Cells successfully transfected with the DNG$_{\alpha q}$ were then identified based on their expression of EGFP. Transfection of the DNG$_{\alpha q}$ ($n=6$) in hTM cells resulted in a significant reduction in the WIN55,212-2-mediated [Ca^{2+}]$_i$ increase compared with mock transfection ($P<0.01$, $n=12$) and empty pIRES2-EGFP vector ($P<0.05$, $n=3$). The activity of the DNG$_{\alpha q}$ was also verified using 10 μM ATP, which produced a significant ($P<0.01$, $n=7$) reduction in the amplitude of the ATP-mediated increase in [Ca^{2+}]$_i$ (data not shown).

WIN55,212-2 activates MAPK via CB$_1$-G$_{i/o}$ coupling

The most widely reported signalling mechanism for CB$_1$ involves coupling to members of the PTX-sensitive G$_{i/o}$ protein family to inhibit adenylyl cyclase and activate the MAPK pathway (Howlett, 2005). Western blotting revealed WIN55,212-2 activation of the MAPK pathway (Figures 5a and b) with a concentration-dependent increase in ERK1/2 phosphorylation (pERK). In-Cell Western analysis demonstrated that the WIN55212-2-mediated increase in pERK was blocked by PTX and the CB$_1$ antagonist, AM251. Figures 5c–e show relative pERK (as a ratio of total ERK) in cells treated with no agonist (0.1% DMSO) and with 5–10 μM WIN55,212-2 or CP55940. 10 μM AM251 inhibited the WIN55,212-2-mediated increase in pERK, at 5 μM ($P<0.05$, $n=16$) and 10 μM ($P<0.001$, $n=14$), confirming the activity of CB$_1$. Figure 5d reveals that the WIN55,212-2-mediated increase in pERK is inhibited by pretreatment with 500 ng ml^{-1} PTX (5 μM, $P<0.01$, $n=8$; 10 μM, $P<0.001$, $n=8$). There is a substantial reduction in both the EC$_{50}$ and E$_{max}$ obtained using In-Cell Western analysis in comparison with traditional western blot. This is probably the result of differing levels of nonspecific binding between the pERK2 and ERK2 antibodies. The nonspecific binding is negated when proteins are resolved on a gel (Figure 5a); however, it will
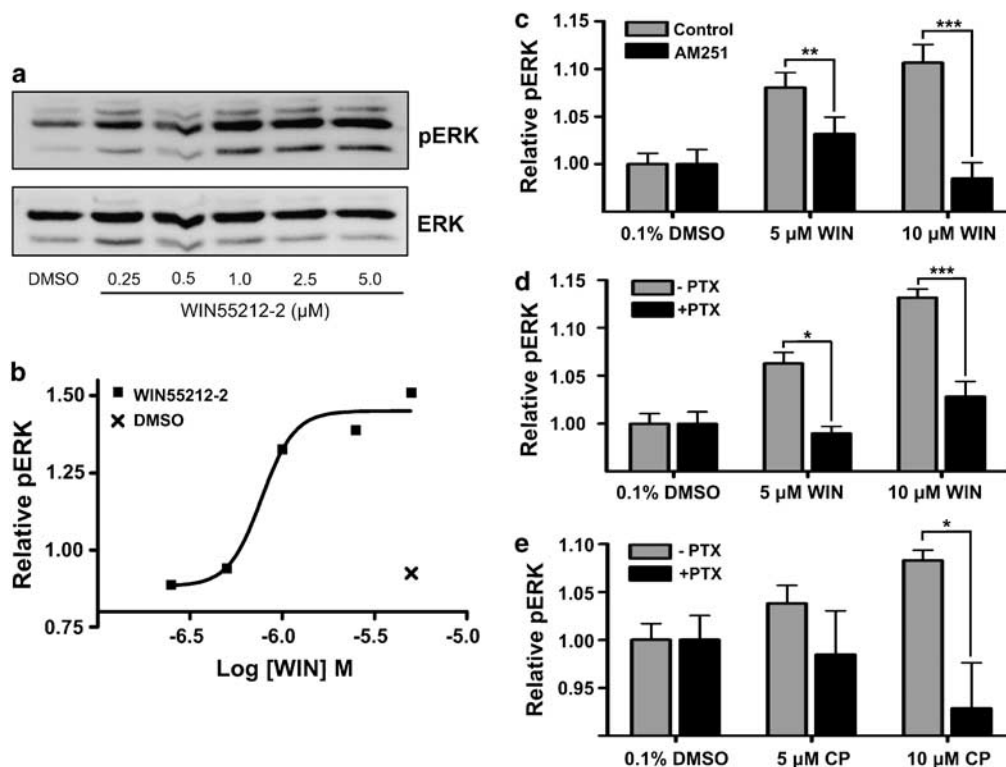
Figure 5 WIN55,212-2 activation of MAP kinase pathway is a result of CB$_1$-G$_{i/o}$ signal transduction. Figures show the increase in phosphorylation of extracellular signal-regulated kinase 2 (pERK2) following a 5 min exposure to WIN55,212-2 or CP55940 using Western blot (**a** and **b**) and infrared In-Cell Western analysis (**c–e**). pERK2 levels were normalized to total ERK2 protein and expressed as relative pERK. (**a**) Western blot showing concentration effect of WIN55,212-2 treatment (0.25–5 μM). (**b**) Relative pERK2 following densitometric quantification of western blot. (**c**) Increase in pERK with 5–10 μM WIN55,212-2 in the presence and absence of 10 μM AM251 ($n=16$). (**d**) Increase in pERK with 5–10 μM WIN55,212-2 with and without PTX pretreatment ($n=8$). (**e**) Increase in pERK with 5–10 μM CP55940 with and without PTX pretreatment ($n=8$). Results are normalized to 0.1% DMSO control treatments. *$P<0.05$, **$P<0.01$ and ***$P<0.001$. PTX, pertussis toxin; DMSO, dimethylsulphoxide.

contribute to the overall signal obtained with In-Cell Western analysis. Figure 5e shows relative pERK following treatment with 5 and 10 μM CP55940 with and without PTX pretreatment. PTX reduced the CP55940-mediated increase in pERK at 10 μM ($P < 0.05$, $n = 8$).

Discussion

Our study demonstrates that activation of CB$_1$ in hTM cells results in increases in $[Ca^{2+}]_i$ and ERK1/2 phosphorylation via agonist-dependent coupling to both G$_{q/11}$ and G$_{i/o}$ signalling pathways. While cannabinoid agonists have been implicated in CB$_1$-mediated increases in $[Ca^{2+}]_i$ in a variety of cell types (Howlett, 2005), the majority of these studies identified the involvement of G$_{i/o}$ proteins, which are capable of mobilizing Ca^{2+} via βγ-subunit activation of PLC (Sugiura *et al.*, 1996; Netzeband *et al.*, 1999; Rubovitch *et al.*, 2004). Our results show that in hTM cells, the WIN55,212-2-induced increase in $[Ca^{2+}]_i$ was insensitive to PTX, and is therefore independent of G$_{i/o}$ coupling, but was abolished using transient transfection of a DNG$_{αq}$ subunit. This DNG$_{αq}$ has been demonstrated to inhibit the WIN55,212-2-mediated increase in $[Ca^{2+}]_i$ in HEK293 cells expressing rat CB$_1$ (Lauckner *et al.*, 2005). In contrast to WIN55,212-2, the $[Ca^{2+}]_i$ increase mediated by CP55940 in hTM cells was PTX-sensitive, indicative of CB$_1$-G$_{i/o}$ coupling. Furthermore, CP55940 was less potent and significantly less efficacious than WIN55,212-2 in increasing $[Ca^{2+}]_i$. The eicosanoid, methanandamide, failed to increase $[Ca^{2+}]_i$ in hTM cells at doses that both WIN55,212-2 and CP55940 evoked a Ca^{2+} increase, suggesting that this agonist had reduced potency at CB$_1$ for coupling to either G$_{q/11}$ or G$_{i/o}$ to increase $[Ca^{2+}]_i$ in hTM cells.

In hTM cells, WIN55,212-2 activation of endogenous CB$_1$-G$_{q/11}$ signalling involved activation of PLC and mobilization of Ca^{2+} from thapsigargin and cyclopiazonic acid-sensitive intracellular stores. The possibility of WIN55,212-2 increasing Ca^{2+} in hTM cells through direct inhibition of the sarcoplasmic/endoplasmic reticulum Ca^{2+} ATPase pumps is unlikely as hTM cells were still able to respond to 10 μM ATP with an increase in Ca^{2+} following exposure to WIN55,212-2 (data not shown), a process that is known to require intact Ca^{2+} stores (von Kügelgen and Wetter, 2000).

We observed no significant difference in the amplitude of the WIN55,212-2-mediated Ca^{2+} increase in cells pretreated with PTX in comparison with controls. This is in contrast to CB$_1$-expressing HEK293 cells, which have been shown to produce a significantly greater WIN55,212-2-mediated Ca^{2+} response following PTX treatment (Lauckner *et al.*, 2005). The reason for this discrepancy may reflect receptor density and the level of constitutive activity and/or composition of the intracellular milieu: endogenously expressed CB$_1$ exists in a system where the molecular stoichiometry of receptor, G-protein, and effectors are dramatically different from those of heterologous expression systems.

We also observed WIN55,212-2-mediated phosphorylation of ERK1/2 in hTM cells. In contrast to the WIN55,212-2-mediated $[Ca^{2+}]_i$ increase, WIN55,212-2-mediated ERK1/2 phosphorylation was PTX-sensitive, suggesting CB$_1$-G$_{i/o}$

signalling. We further investigated the possibility that WIN55,212-2 could be acting at both CB$_1$ and CB$_2$ receptors to activate pERK, a reasonable scenario given the affinity of WIN55,212-2 for both CB$_1$ and CB$_2$ and the identification of functional CB$_2$ receptors in porcine TM (Zhong *et al.*, 2005). However; the WIN55,212-2-mediated increase in pERK resulted from CB$_1$ activation since it was inhibited by AM251, a compound that acts as either a neutral antagonist or an inverse agonist at CB$_1$ (Pertwee, 2005a). CP55940 was also able to increase pERK and, like WIN55,212-2, exhibited greater potency in hTM cells with respect to ERK phosphorylation than that observed for CB$_1$-mediated $[Ca^{2+}]_i$ increases. Differential potency has been previously reported in WIN55,212-2 selectivity for different G$_{i/o}$ protein subunits (Prather *et al.*, 2000). Our results further suggest that cannabinoid agonist structure may also play a key role in the coupling of CB$_1$ to G-proteins of both the G$_{q/11}$ and G$_{i/o}$ classes.

Cannabinoid receptor agonists occupy a common binding region within the CB$_1$ receptor, as demonstrated by their mutual competitive displacement in both radioligand binding assays (Showalter *et al.*, 1996; Felder *et al.*, 1998; Horn *et al.*, 2003) and structure–activity relationship modelling (Shim *et al.*, 1998). However; within the hypothesized binding region, mutagenesis (Song and Bonner, 1996; Chin *et al.*, 1998; McAllister *et al.*, 2003) and molecular modelling (Reggio, 2005; Shim and Howlett, 2006) have demonstrated that the aminoalkylindoles interact with a series of residues distinct from those targeted by classical, non-classical and eicosanoid agonists. Thus, WIN55,212-2 may be more efficacious than the non-classical cannabinoid agonist, CP55940, or the eicosanoids, in inducing or stabilizing a CB$_1$ receptor active state that is capable of recruiting G$_{q/11}$ proteins in addition to the preferred G$_{i/o}$ proteins.

The observation of multiple signalling cascades descending from activation of a single receptor type is frequently associated with heterologous expression systems, where the surface expression of the receptor has been increased beyond the normal physiological range (Hermans, 2003). Whether these alterations in receptor density are promoting transduction through atypical pathways, or simply exposing endogenously relevant secondary pathways, remains questionable. This study demonstrates that endogenously expressed CB$_1$ receptors in ocular hTM cells are capable of pleiotropy in signal transduction in an agonist-dependent manner by coupling to either G$_{q/11}$ or G$_{i/o}$ to increase $[Ca^{2+}]_i$ and activate ERK1/2.

Cannabinoid receptors and their endogenous ligands, anandamide/arachidonylethanolamide and 2-AG, are present in tissues of both the anterior and posterior chambers of the mammalian eye (Bisogno *et al.*, 1999; Straiker *et al.*, 1999; Lu *et al.*, 2000; Porcella *et al.*, 2000; Chen *et al.*, 2005). This distribution suggests they may play an important role in a diverse array of ocular functions including IOP regulation (reviewed in Tomida *et al.*, 2004). The physiological importance of the endocannabinoid system in IOP regulation is further emphasized with the finding that 2-AG levels are significantly reduced in human glaucomatous ciliary muscle (Chen *et al.*, 2005). In addition to these findings, endocannabinoids have been postulated to play a neuro-

protective role in a high IOP-induced retina ischaemia model of glaucoma (Nucci *et al.*, 2007). Anandamide/arachidonyl-ethanolamide levels have been found to be increased in cornea, ciliary body, choroid and retina in patients with diabetic retinopathy and age-related macular degeneration (Matias *et al.*, 2006), suggesting other ocular pathologies may also involve alterations in endocannabinoid signalling.

The presence of CB$_1$ receptors in the tissues of both inflow and outflow pathways in the eye (Straiker *et al.*, 1999; Porcella *et al.*, 2000; Stamer *et al.*, 2001) indicates that activation of CB$_1$ at multiple sites probably contributes to a net decrease in IOP. Consistent with this, changes in aqueous inflow (Chien *et al.*, 2003) and outflow (Colasanti, 1990; Beilin *et al.*, 2000) have been observed following cannabinoid administration. Although cannabinoid actions on individual tissues of the outflow pathway have not been extensively examined, a study in ciliary muscle, a tissue that is responsible for accommodation of the lens and traction on the TM, has demonstrated that the cannabinoid agonists, CP55940 and anandamide/arachidonylethanolamide, mediated Ca^{2+}-dependent contraction of the ciliary muscle via a PTX-sensitive G$_{i/o}$ signalling pathway (Lograno and Romano, 2004). In primate eye it has been demonstrated that agonists that contract the ciliary muscle can expand the TM and reduce outflow resistance, thus contributing to a decrease in IOP (Lütjen-Drecoll, 1998). In hTM tissue, CB$_1$-induced increases in Ca^{2+} may also lead to alterations in TM contractility and outflow resistance via activation of Ca^{2+}-dependent pathways or Ca^{2+}-sensitive ion channels (Thieme *et al.*, 2001; Stumpff *et al.*, 2005). Additionally, activation of ERK1/2 in TM cells has been associated with an increase in the synthesis and release of matrix metalloproteinase-2 (Shearer and Crosson, 2001), an enzyme believed to be involved in augmenting aqueous humour outflow (Okada *et al.*, 1998). Our data in hTM cells suggest that agonist-specific CB$_1$ signal transduction may contribute to differences in the efficacy of different classes of cannabinoid ligands to alter TM function. Consideration of this may have therapeutic consequences for the design of novel cannabinoid agents targeted as ocular hypotensive drugs.

Acknowledgements

Conflict of interest

The authors state no conflict of interest.

References

Beilin M, Neumann R, Belkin M, Green K, Bar-Ilan A (2000). Pharmacology of the intraocular pressure (IOP) lowering effect of systemic dexanabinol (HU-211), a non-psychotropic cannabinoid. *J Ocul Pharmacol Ther* **6**: 217–230.

Berridge M (1993). Inositol trisphosphate and calcium signalling. *Nature* **361**: 315–325.

Bisogno T, Delton-Vandenbroucke I, Milone A, Lagarde M, Di Marzo V (1999). Biosynthesis and inactivation of N-arachidonoyletha-nolamine (anandamide) and N-docosahexaenoylethanolamine in bovine retina. *Arch Biochem Biophys* **370**: 300–307.

Bonhaus D, Chang L, Kwan J, Martin G (1998). Dual activation and inhibition of adenylyl cyclase by cannabinoid receptor agonists: evidence for agonist-specific trafficking of intracellular responses. *J Pharmacol Exp Ther* **287**: 884–888.

Chen J, Matias I, Dinh T, Lu T, Venezia S, Nieves A *et al.* (2005). Finding of endocannabinoids in human eye tissues: implications for glaucoma. *Biochem Biophys Res Commun* **330**: 1062–1067.

Chien FY, Wang R-F, Mittag TW, Podos SM (2003). Effect of WIN 55212-2, a cannabinoid receptor agonist, on aqueous humor dynamics in monkeys. *Arch Ophthalmol* **121**: 87–90.

Chin C, Lucas-Lenard J, Abadji V, Kendall DA (1998). Ligand binding and modulation of cyclic AMP levels depend on the chemical nature of residue 192 of the human cannabinoid receptor 1. *J Neurochem* **70**: 366–373.

Colasanti B (1990). A comparison of the ocular and central effects of Δ^9-tetrahydrocannabinol and cannabigerol. *J Ocul Pharmacol Ther* **6**: 259–269.

Felder C, Joyce K, Briley E, Glass M, Mackie K, Fahey K *et al.* (1998). LY320135, a novel cannabinoid CB$_1$ receptor antagonist, unmasks coupling of the CB$_1$ receptor to stimulation of cAMP accumulation. *J Pharmacol Exp Ther* **284**: 291–297.

Felder C, Joyce K, Briley E, Mansouri J, Mackie K, Blond O *et al.* (1995). Comparison of the pharmacology and signal transduction of the human cannabinoid CB$_1$ and CB$_2$ receptors. *Mol Pharmacol* **48**: 443–450.

Ferrer E (2006). Trabecular meshwork as a new target for the treatment of glaucoma. *Drug News Perspect* **19**: 151–158.

Glass M, Felder C (1997). Concurrent stimulation of cannabinoid CB$_1$ and dopamine D$_2$ receptors augments cAMP accumulation in striatal neurons: evidence for a G$_s$ linkage to the CB$_1$ receptor. *J Neurosci* **17**: 5327–5333.

Glass M, Northup JK (1999). Agonist selective regulation of G proteins by cannabinoid CB$_1$ and CB$_2$ receptors. *Mol Pharmacol* **56**: 1362–1369.

Hepler R, Frank I (1971). Marihuana smoking and intraocular pressure. *JAMA* **217**: 1392.

Hermans E (2003). Biochemical and pharmacological control of the multiplicity of coupling at G-protein-coupled receptors. *Pharmacol Ther* **99**: 25–44.

Horn F, Bettler E, Oliveira L, Campagne F, Cohen FE, Vriend G (2003). GPCRDB information system for G protein-coupled receptors. *Nucl Acids Res* **31**: 294–297.

Howlett A (2005). Cannabinoid receptor signaling. In: Pertwee R (eds). *Cannabinoids*. Springer-Verlag: Berlin. pp 53–79.

Jan C-R, Ho C-M, Wu S-N, Tseng C-J (1998). The phospholipase C inhibitor U73122 increases cytosolic calcium in MDCK cells by activating calcium influx and releasing stored calcium. *Life Sci* **63**: 895–908.

Jonsson K-O, Holt S, Fowler CJ (2006). The endocannabinoid system: current pharmacological research and therapeutic possibilities. *Basic Clin Pharmacol Toxicol* **98**: 124–134.

Kaufman P, Gabelt B, Tian B, Liu X (1999). Advances in glaucoma diagnosis and therapy for the next millennium: new drugs for trabecular and uveoscleral outflow. *Semin Ophthalmol* **14**: 130–143.

Lauckner JE, Hille B, Mackie K (2005). The cannabinoid agonist WIN55,212-2 increases intracellular calcium via CB$_1$ receptor coupling to G$_{q/11}$ G proteins. *Proc Natl Acad Sci USA* **102**: 19144–19149.

Lograno MD, Romano MR (2004). Cannabinoid agonists induce contractile responses through G$_{i/o}$-dependent activation of phospholipase C in the bovine ciliary muscle. *Eur J Pharmacol* **494**: 55–62.

Lu Q, Straiker A, Lu Q, Maguire G (2000). Expression of CB$_2$ cannabinoid receptor mRNA in adult rat retina. *Vis Neurosci* **17**: 91–95.

Lütjen-Drecoll E, Wiendl H, Kaufman P (1998). Acute and chronic structural effects of pilocarpine on monkey outflow tissues. *Trans Am Ophthalmol Soc* **96**: 171–195.

Matias I, Wang JW, Moriello AS, Nieves A, Woodward DF, Di Marzo V (2006). Changes in endocannabinoid and palmitoylethanolamide levels in eye tissues of patients with diabetic retinopathy and age-related macular degeneration. *Prostaglandins Leukot Essent Fatty Acids* **75**: 413–418.

Matsuda LA, Lolait SJ, Brownstein MJ, Young AC, Bonner TI (1990). Structure of a cannabinoid receptor and functional expression of the cloned cDNA. *Nature* **346**: 561–564.

McAllister SD, Rizvi G, Anavi-Goffer S, Hurst DP, Barnett-Norris J, Lynch DL *et al.* (2003). An aromatic microdomain at the cannabinoid CB$_1$ receptor constitutes an agonist/inverse agonist binding region. *J Med Chem* **46**: 5139–5152.

Mogami H, Mills CL, Gallacher DV (1997). Phospholipase C inhibitor, U73122, releases intracellular Ca^{2+}, potentiates Ins(1,4,5)P3-mediated Ca^{2+} release and directly activates ion channels in mouse pancreatic acinar cells. *Biochem J* **324**: 645–651.

Munro S, Thomas KL, Abu-Shaar M (1993). Molecular characterization of a peripheral receptor for cannabinoids. *Nature* **365**: 61–65.

Netzeband JG, Conroy SM, Parsons KL, Gruol DL (1999). Cannabinoids enhance NMDA-elicited Ca^{2+} signals in cerebellar granule neurons in culture. *J Neurosci* **19**: 8765–8777.

Nucci C, Gasperi V, Tartaglione R, Cerulli A, Terrinoni A, Bari M *et al.* (2007). Involvement of the endocannabinoid system in retinal damage after high intraocular pressure-induced ischemia in rats. *Invest Ophthalmol Vis Sci* **48**: 2997–3004.

Okada Y, Matsuo T, Ohtsuki H (1998). Bovine trabecular cells produce TIMP-1 and MMP-2 in response to mechanical stretching. *Jpn J Ophthalmol* **42**: 90–94.

Pertwee R (2005a). Inverse agonism and neutral antagonism at cannabinoid CB$_1$ receptors. *Life Sci* **76**: 1307–1324.

Pertwee RG (2005b). Pharmacological actions of cannabinoids. In: Pertwee RG (eds). *Cannabinoids*. Springer-Verlag: Berlin. pp 1–51.

Pinton P, Pozzan T, Rizzuto R (1998). The Golgi apparatus is an inositol 1,4,5-trisphosphate-sensitive Ca^{2+} store, with functional properties distinct from those of the endoplasmic reticulum. *EMBO J* **17**: 5298–5308.

Piomelli D (2003). The molecular logic of endocannabinoid signalling. *Nat Rev Neurosci* **4**: 873–884.

Porcella A, Maxia C, Gessa GL, Pani L (2000). The human eye expresses high levels of CB$_1$ cannabinoid receptor mRNA and protein. *Eur J Neurosci* **12**: 1123–1127.

Prather PL, Martin NA, Breivogel CS, Childers SR (2000). Activation of cannabinoid receptors in rat brain by WIN 55212-2 produces coupling to multiple G protein alpha-subunits with different potencies. *Mol Pharmacol* **57**: 1000–1010.

Reggio P (2005). Cannabinoid receptors and their ligands: ligand–ligand and ligand-receptor modeling approaches. In: Pertwee R (eds). Cannabinoids: Springer-Verlag, Berlin. pp 247–281.

Rubovitch V, Gafni M, Sarne Y (2004). The involvement of VEGF receptors and MAPK in the cannabinoid potentiation of Ca^{2+} flux into N18TG2 neuroblastoma cells. *Brain Res Mol Brain Res* **120**: 138–144.

Shearer T, Crosson CE (2001). Activation of extracellular signal-regulated kinase in trabecular meshwork cells. *Exp Eye Res* **73**: 25–35.

Shim J, Collantes E, Welsh W, Subramaniam B, Howlett A, Eissenstat M *et al.* (1998). Three-dimensional quantitative structure–activity relationship study of the cannabimimetic (aminoalkyl)indoles using comparative molecular field analysis. *J Med Chem* **41**: 4521–4532.

Shim J, Howlett A (2006). WIN55212-2 docking to the CB$_1$ cannabinoid receptor and multiple pathways for conformational induction. *J Chem Inf Model* **46**: 1286–1300.

Showalter V, Compton D, Martin B, Abood M (1996). Evaluation of binding in a transfected cell line expressing a peripheral cannabinoid receptor (CB$_2$): identification of cannabinoid receptor subtype selective ligands. *J Pharmacol Exp Ther* **278**: 989–999.

Song Z, Bonner T (1996). A lysine residue of the cannabinoid receptor is critical for receptor recognition by several agonists but not WIN55212-2. *Mol Pharmacol* **49**: 891–896.

Stamer WD, Golightly SF, Hosohata Y, Ryan EP, Porter AC, Varga E *et al.* (2001). Cannabinoid CB$_1$ receptor expression, activation and detection of endogenous ligand in trabecular meshwork and ciliary process tissues. *Eur J Pharmacol* **431**: 277–286.

Straiker AJ, Maguire G, Mackie K, Lindsey J (1999). Localization of cannabinoid CB$_1$ receptors in the human anterior eye and retina. *Invest Ophthalmol Vis Sci* **40**: 2442–2448.

Stumpff F, Boxberger M, Krauss A, Rosenthal R, Meissner S (2005). Stimulation of cannabinoid (CB$_1$) and prostanoid (EP2) receptors opens BKCa channels and relaxes ocular trabecular meshwork. *Exp Eye Res* **80**: 697–708.

Sugiura T, Kodaka T, Kondo S, Tonegawa T, Nakane S, Kishimoto S *et al.* (1996). 2-Arachidonoylglycerol, a putative endogenous cannabinoid receptor ligand, induces rapid, transient elevation of intracellular free Ca^{2+} in neuroblastoma × glioma hybrid NG108-15 cells. *Biochem Biophys Res Commun* **229**: 58–64.

Tan J, Peters D, Kaufman P (2006). Recent developments in understanding the pathophysiology of elevated intraocular pressure. *Curr Opin Ophthalmol* **17**: 168–174.

Thieme H, Stumpff F, Ottlecz A, Percicot CL, Lambrou GN, Wiederholt M (2001). Mechanisms of action of unoprostone on trabecular meshwork contractility. *Invest Ophthalmol Vis Sci* **42**: 3193–3201.

Tomida I, Pertwee RG, Azuara-Blanco A (2004). Cannabinoids and glaucoma. *Br J Ophthalmol* **88**: 708–713.

Treiman M, Caspersen C, Christensen SB (1998). A tool coming of age: thapsigargin as an inhibitor of sarco-endoplasmic reticulum Ca^{2+}-ATPases. *Trends Pharmacol Sci* **19**: 131–135.

Urban JD, Clarke WP, von Zastrow M, Nichols DE, Kobilka B, Weinstein H *et al.* (2007). Functional selectivity and classical concepts of quantitative pharmacology. *J Pharmacol Exp Ther* **320**: 1–13.

von Kügelgen I, Wetter A (2000). Molecular pharmacology of P2Y-receptors. *Naunyn Schmiedebergs Arch Pharmacol* **362**: 310–323.

Werry T, Wilkinson G, Willars G (2003). Mechanisms of cross-talk between G-protein-coupled receptors resulting in enhanced release of intracellular Ca^{2+}. *Biochem J* **374**: 281–296.

Willems P, Put FVd, Engbersen R, Bosch R, Hoof HV, Pont Jd (1994). Induction of Ca^{2+} oscillations by selective, U73122-mediated, depletion of inositol-trisphosphate-sensitive Ca^{2+} stores in rabbit pancreatic acinar cells. *Pfluegers Arch* **427**: 233–243.

Yu B, Simon MI (1998). Interaction of the xanthine nucleotide binding Gαo mutant with G protein-coupled receptors. *J Biol Chem* **273**: 30183–30188.

Zhong L, Geng L, Njie Y, Feng W, Song Z-H (2005). CB$_2$ cannabinoid receptors in trabecular meshwork cells mediate JWH015-induced enhancement of aqueous humor outflow facility. *Invest Ophthalmol Vis Sci* **46**: 1988–1992.